

Magnetic transitions and magnetostrictive properties of $\text{Tb}_x\text{Dy}_{1-x}(\text{Fe}_{0.8}\text{Co}_{0.2})_2$ ($0.20 \leq x \leq 0.40$)

Jin-jun Liu, Wei-jun Ren,* Da Li, Nai-kun Sun, Xin-guo Zhao, Ji Li, and Zhi-dong Zhang
*Shenyang National Laboratory for Materials Science, Institute of Metal Research and International Centre for Materials Physics,
 Chinese Academy of Sciences, Shenyang, 110016, People's Republic of China*

(Received 27 October 2006; revised manuscript received 26 December 2006; published 28 February 2007)

The magnetic transitions and magnetic and magnetostrictive properties of $\text{Tb}_x\text{Dy}_{1-x}(\text{Fe}_{0.8}\text{Co}_{0.2})_2$ ($0.20 \leq x \leq 0.40$) compounds have been investigated. The spin-reorientation temperature T_{SR} decreases from above to below room temperature, when x is increased from 0.25 to 0.40. The easy magnetization direction at room temperature of the Laves phase lies along the $\langle 100 \rangle$ axis in compounds with $0.20 \leq x \leq 0.27$, while it lies along the $\langle 111 \rangle$ axis as $0.30 \leq x \leq 0.40$. The magnetocrystalline anisotropy constant K_1 at room temperature reaches a minimum value at $x=0.30$, indicating it is near the composition for anisotropy compensation. The large polycrystalline saturation magnetostriction $\lambda_s \approx 980$ ppm is observed for $x=0.30$, which can be ascribed to the large magnetostriction coefficients λ_{111} and λ_{100} . λ_{100} has a value larger than 600 ppm for the compounds with $0.30 \leq x \leq 0.35$, which can be attributed to the change of the filling of the $3d$ band due to Co substitution for Fe. $\text{Tb}_{0.30}\text{Dy}_{0.70}(\text{Fe}_{0.8}\text{Co}_{0.2})_2$ with a high magnetostriction and a low anisotropy is found to be a good candidate material for magnetostriction applications. A detailed spin configuration diagram for $\text{Tb}_x\text{Dy}_{1-x}(\text{Fe}_{0.8}\text{Co}_{0.2})_2$ Laves phase around the composition for the anisotropy compensation is given, which should be a guide to develop novel magnetostrictive materials for applications in this series.

DOI: 10.1103/PhysRevB.75.064429

PACS number(s): 75.80.+q, 74.25.Ha

I. INTRODUCTION

For practical applications of magnetostrictive materials, high strains at low fields are necessary so that a minimum in anisotropy is required. The pseudobinary compound $\text{Tb}_{0.27}\text{Dy}_{0.73}\text{Fe}_2$ (Terfenol-D) was found to be such an excellent material, owing to its large magnetostriction and its spin-reorientation temperature (T_{SR}) near to room temperature.¹ Thereafter, a large amount of research work has been done on the substitution of other $3d$ metals such as Co, Ni, and Mn for Fe in Terfenol-D, in an effort to further improve its magnetic and magnetostrictive properties.²⁻⁶ It was found that Mn or Ni substitution for Fe causes a decrease of the Curie temperature T_C , while a small amount of Co substitution increases the Curie temperature.²⁻⁵ Nevertheless, almost all of these substitutions decrease the magnetostriction of Terfenol-D at room temperature, resulting from the fact that the substitutions change the spin-reorientation temperature T_{SR} and increase the anisotropy of Terfenol-D. Usually, the magnetocrystalline anisotropies of rare-earth ions are larger than those of the $3d$ transition-metal ions in $R\text{Fe}_2$ compounds. The magnetocrystalline anisotropies of the $R\text{Fe}_2$ compounds are practically dominated by the rare-earth ions. However, the magnetocrystalline anisotropy of Terfenol-D is small due to the anisotropy compensation between Tb^{3+} with a negative anisotropy constant K_1 and Dy^{3+} ion with a positive anisotropy constant K_1 . Thus, it is reasonable that the substitution of $3d$ -metal elements in Terfenol-D could contribute significantly to its anisotropy.⁶ It has been pointed out that Co substitution increases while Mn substitution decreases the spin-reorientation temperature T_{SR} .^{4,7} Considering the anisotropy nature of Tb^{3+} (decreasing T_{SR}) and Dy^{3+} ion (increasing T_{SR}), Clark *et al.* deemed an improved magnetostrictive material containing Co could be formed, which should have an optimum performance at room temperature.⁴ In fact, it is necessary to increase the Tb content in Co-

modified Terfenol-D to maintain the spin-reorientation temperature T_{SR} near room temperature. It has been demonstrated by Guo *et al.* that the composition for the anisotropy compensation in $\text{Tb}_{1-x}\text{Dy}_x(\text{Fe}_{0.8}\text{Co}_{0.2})_2$ is shifted to the Tb-rich side compared with Terfenol-D.⁸ As is known, magnetostrictive materials containing more Tb content should have a larger magnetostriction. However, Guo *et al.* did not observe a large magnetostriction around the composition for anisotropy compensation in applied magnetic fields.⁸ This might be due to the fact that there were too few experimental points so that the appropriate composition for the anisotropy compensation was missing, since the magnetostrictive properties are very sensitive to the composition, especially the Tb/Dy ratio.⁹ Thus, a detailed investigation of the $\text{Tb}_x\text{Dy}_{1-x}(\text{Fe}_{0.8}\text{Co}_{0.2})_2$ alloys near the composition for anisotropy compensation is crucial to develop new magnetostrictive materials for applications. In this work, the spin configuration, magnetic transitions, magnetic properties, anisotropy compensation, and magnetostriction of $\text{Tb}_x\text{Dy}_{1-x}(\text{Fe}_{0.8}\text{Co}_{0.2})_2$ ($0.20 \leq x \leq 0.40$) compounds are investigated in detail. A large magnetostriction induced by applied magnetic fields is obtained, not only because of the small anisotropy led by the anisotropy compensation among the different elements, but also a large magnetostriction coefficient λ_{100} originating from the change of the filling of the $3d$ -band system due to the Co substitution for Fe. $\text{Tb}_{0.30}\text{Dy}_{0.70}(\text{Fe}_{0.8}\text{Co}_{0.2})_2$ compound with a high magnetostriction and a low anisotropy is found to be a good candidate material for magnetostriction applications.

II. EXPERIMENTAL PROCEDURES

All polycrystalline samples of $\text{Tb}_x\text{Dy}_{1-x}(\text{Fe}_{0.8}\text{Co}_{0.2})_2$ alloys with $x=0.20, 0.25, 0.27, 0.30, 0.32, 0.35, 0.38,$ and 0.40 were prepared by arc melting the appropriate constituent metals in a high-purity argon atmosphere. The purities of the

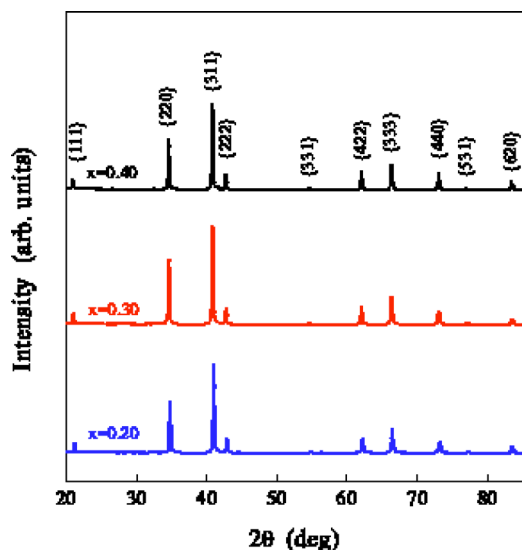


FIG. 1. (Color online) X-ray diffraction patterns of the $\text{Tb}_x\text{Dy}_{1-x}(\text{Fe}_{0.8}\text{Co}_{0.2})_2$ compounds for $x=0.2, 0.30, 0.40$.

constituents are 99.9% for Tb and Dy and 99.8% for Fe and Co. The ingots were homogenized at 820 °C for 7 days in a high-purity argon atmosphere. X-ray diffraction (XRD) was implemented at room temperature with $\text{Cu } K\alpha$ radiation in a Rigaku D/max-2500pc diffractometer equipped with a graphite monochromator. In order to study the easy magnetization direction (EMD) and magnetostriction coefficient λ_{111} of the Laves phases, a high-precision XRD step scanning was performed on powdered samples for the $\{440\}$ peaks of the Laves phase. The effect of the $K\alpha_2$ radiation was eliminated by a standard process. The XRD peaks were fitted by using the fitting function Pearson VII provided by Jade 6.5 XRD analytical software (Materials Data, Inc., Livermore, CA). The temperature dependences of the ac initial susceptibility were recorded by a superconducting quantum interference device (SQUID) magnetometer to detect the spin-reorientation temperature T_{SR} .¹⁰ Magnetization curves at room temperature were measured by the SQUID magnetometer at fields up to 50 kOe. The magnetostriction at room temperature was measured either parallel or perpendicular to the applied field using a standard strain gauge technique.

III. RESULTS AND DISCUSSION

XRD analysis confirms that the homogenized samples of $\text{Tb}_x\text{Dy}_{1-x}(\text{Fe}_{0.8}\text{Co}_{0.2})_2$ ($0.20 \leq x \leq 0.40$) alloys are essentially the single (Tb, Dy)(Fe, Co)₂ phases with a MgCu_2 -type cubic structure over the whole concentration range investigated (some examples are shown in Fig. 1). All the XRD peaks of the compounds slightly shift to lower Bragg angles with increasing Tb content, because of the increase of the lattice constant due to the larger radius of the Tb ion. It is known that spontaneous magnetostriction leads to crystal-structural distortion of the compound with the cubic MgCu_2 -type Laves structure when it is cooled down below its Curie temperature. If the EMD lies along $\langle 111 \rangle$, a rhombohedral distortion caused by magnetostriction will occur; if the EMD

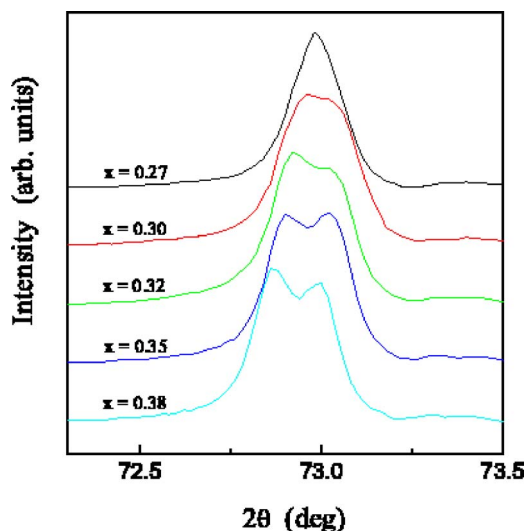


FIG. 2. (Color online) The profiles of the step-scanned $\{440\}$ XRD reflection of the Laves phase in $\text{Tb}_x\text{Dy}_{1-x}(\text{Fe}_{0.8}\text{Co}_{0.2})_2$ alloys.

lies along $\langle 100 \rangle$, a tetrahedral distortion will occur. Usually, these distorted compounds can be classified as a pseudocubic structure, since their structures do not drastically change. The indices $\{hkl\}$ of the pseudocubic Laves phase are also indexed in Fig. 1. Cullen and Clark suggested that the magnetostriction in $R\text{Fe}_2$ Laves compounds is highly anisotropic.¹¹ A large magnetostriction exists when EMD is along $\langle 111 \rangle$, but the magnetostriction is small when EMD is along $\langle 100 \rangle$. Thus, the $\{440\}$ reflection in the XRD pattern is doubly split when EMD lies along $\langle 111 \rangle$, while it keeps a single peak when EMD lies along $\langle 100 \rangle$.^{12,13} In this work, the $\{440\}$ XRD reflection of the $\text{Tb}_x\text{Dy}_{1-x}(\text{Fe}_{0.8}\text{Co}_{0.2})_2$ compounds was step scanned, in order to study EMD and spontaneous magnetostriction. The profile of the $\{440\}$ reflection, which was deduced from $K\alpha_2$ with a standard method, is represented in Fig. 2. Each of the $\{440\}$ reflections forms a single peak when $x \leq 0.27$. Although the tetrahedral distortion caused by magnetostriction is not as small as in the Co-free $R\text{Fe}_2$ compounds, it is still not large enough to be identified by XRD (see the discussion thereafter), suggesting that the EMD of the Laves phase in those compounds lies along $\langle 100 \rangle$. The double splitting of the $\{440\}$ reflection is observed when $x \geq 0.30$, indicating that the EMD of the Laves phase lies along $\langle 111 \rangle$. The double reflections for $x=0.30$ change to a single reflection for $x=0.27$, indicating that the composition anisotropy compensation point at room temperature is in the range of $0.27 \leq x \leq 0.30$, within which the large rhombohedral distortion disappears.

The magnetostriction of the $\text{Tb}_x\text{Dy}_{1-x}(\text{Fe}_{0.8}\text{Co}_{0.2})_2$ compounds was measured in the direction parallel and perpendicular to the applied fields up to 12 kOe. Figure 3 represents the polycrystalline magnetostriction $\lambda_a = \lambda_{\parallel} - \lambda_{\perp}$ as a function of the external magnetic field at room temperature. It is obvious that the saturation is not achieved for all compounds. For isotropic polycrystalline materials, the saturation value λ_{0s} for $\lambda_a = \lambda_{\parallel} - \lambda_{\perp}$ was achieved by an approximate approach for the saturation relation $\lambda_a = \lambda_{0s}(1 - a/H - b/H^2)$, where a and b are constants.¹⁴ The saturation magnetostriction λ_s was

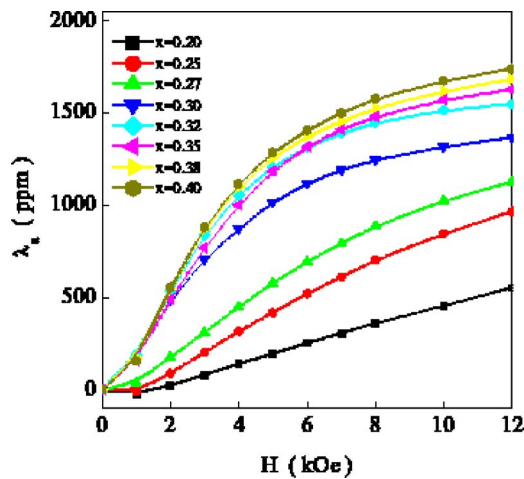


FIG. 3. (Color online) Magnetic field dependence of magnetostriction $\lambda_s (= \lambda_{\parallel} - \lambda_{\perp})$ for the $\text{Tb}_x\text{Dy}_{1-x}(\text{Fe}_{0.8}\text{Co}_{0.2})_2$ compounds.

obtained by the relation $\lambda_s = 2/3\lambda_{0s}$. The composition dependence of the saturation magnetostriction λ_s is plotted in Fig. 4. It is found that there is an increase in the saturation magnetostriction with increasing Tb content. It is reasonable that a Tb ion generates a larger magnetostriction than a Dy ion.

The magnetostriction coefficient λ_{111} of the Laves phase in which the EMD is along $\langle 111 \rangle$ can be calculated by the splitting of the $\{440\}$ reflections, as shown in Fig. 2, by using the following equation:^{15,16}

$$\lambda_{111} = 2 \frac{d_{404} - d_{40\bar{4}}}{d_{404} + d_{40\bar{4}}}, \quad (1)$$

where d_{404} and $d_{40\bar{4}}$ denote the crystallographic plane distances in pseudocubic indices (hkl) . The XRD patterns for both powder and bulk samples confirm that the grains are randomly distributed in the polycrystalline samples. The magnetostriction constant λ_{100} of the samples can be derived from the relation $\lambda_s = 0.6\lambda_{111} + 0.4\lambda_{100}$ of polycrystalline materials with cubic structure.¹⁷ The Tb content dependences of

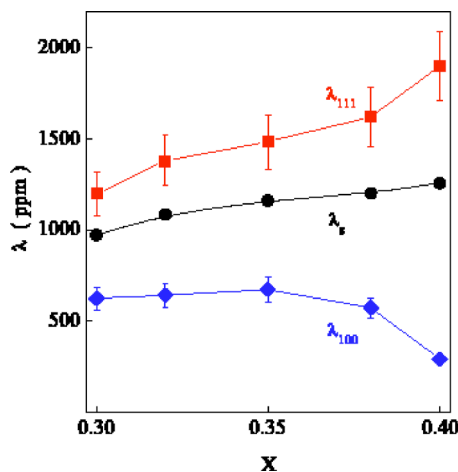


FIG. 4. (Color online) Composition dependence of saturation magnetostriction λ_s and spontaneous magnetostriction λ_{111} and λ_{100} for $\text{Tb}_x\text{Dy}_{1-x}(\text{Fe}_{0.8}\text{Co}_{0.2})_2$ compounds.

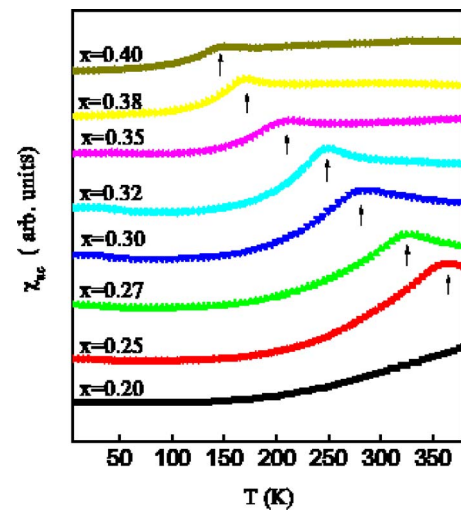


FIG. 5. (Color online) Temperature dependence of the ac initial susceptibility χ_{ac} of the $\text{Tb}_x\text{Dy}_{1-x}(\text{Fe}_{0.8}\text{Co}_{0.2})_2$ compounds. The arrow indicates the spin-reorientation temperature T_{SR} .

the spontaneous magnetostrictions λ_{111} and λ_{100} of the compounds are shown in Fig. 4. λ_{111} increases monotonously with increasing Tb content, while λ_{100} enhances slightly for $x \leq 0.35$ and decreases for $x \geq 0.35$. Unlike Teferol-D where $\lambda_{100} \ll \lambda_{111}$, a relatively large λ_{100} , larger than 600 ppm for $0.30 \leq x \leq 0.35$, is expected, although it cannot be detected directly by XRD. Obviously, the giant saturation magnetostriction $\lambda_s \approx 980$ ppm for $x = 0.30$ and $\lambda_s \approx 1100$ ppm for $x = 0.32$ can be ascribed to the large spontaneous magnetostriction coefficients λ_{111} and λ_{100} .

The atomic model based on the structure of the cubic Laves phase well explained the anisotropy of magnetostriction of $R\text{Fe}_2$ compound.¹¹ The relation $\lambda_{111} \gg \lambda_{100}$ is valid for almost all $R\text{Fe}_2$ series. But the nature of Fe or Co in cubic Laves compounds differs greatly. Fe has an intrinsic moment, whereas Co only has an induced moment. Levitin and Markosyan¹⁸ and Gratz *et al.*¹⁶ investigated the magnetic and the magnetoelastic properties of $R\text{Co}_2$ compounds and found that both λ_{111} and λ_{100} of all $R\text{Co}_2$ compounds investigated possessed a large value at 0 K. Furthermore, λ_{111} as a function of the rare-earth element followed well the theoretical prediction based on the single-ion model, but λ_{100} did not obey this prediction and almost held the value close to that of GdCo_2 .¹ It suggested that λ_{100} was contributed by Co instead of the rare-earth element. A large value for λ_{100} was also observed in $R\text{Fe}_2$ compounds with Mn or Co substitution for Fe.^{5,6,14} In $\text{Tb}(\text{Fe}_{1-x}\text{Mn}_x)_2$, except for a large λ_{100} , a change of the isomer shift was observed by Mössbauer spectra, which seemed to imply that the large λ_{100} origins from the change of the filling of the 3d band.^{5,18} In our present work, 20 at. % Co substitution for Fe changes the filling of the 3d band and its nature, inducing the appearance of a large λ_{100} .

The temperature dependence of the ac initial susceptibility χ_{ac} of the $\text{Tb}_x\text{Dy}_{1-x}(\text{Fe}_{0.8}\text{Co}_{0.2})_2$ compounds is shown in Fig. 5. An anomaly is observed for each alloy with $0.25 \leq x \leq 0.40$, corresponding to a spin-reorientation transition from $\langle 100 \rangle$ to $\langle 111 \rangle$.^{4,10} This is consistent with the XRD results that the EMD of the Laves phase lies along $\langle 111 \rangle$ at

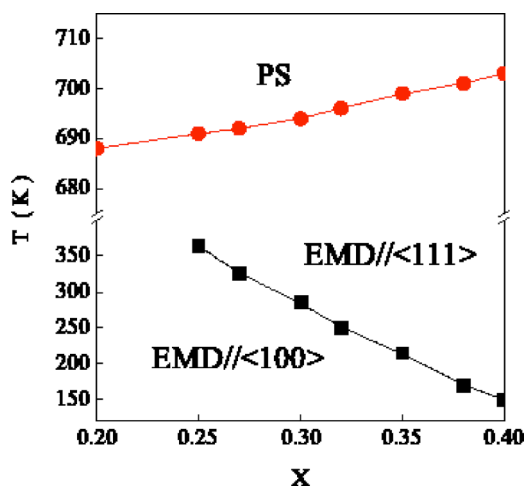


FIG. 6. (Color online) The schematic diagram of the spin configuration for $Tb_xDy_{1-x}(Fe_{0.8}Co_{0.2})_2$ ($0.20 \leq x \leq 0.40$) compounds. The circles, squares, and PS denote the Curie temperature, the spin-reorientation temperature, and the paramagnetic state, respectively.

room temperature when $x \geq 0.30$. No anomaly appears in the temperature variation of χ_{ac} for the $Tb_{0.2}Dy_{0.8}(Fe_{0.8}Co_{0.2})_2$ compound below the maximum available temperature 380 K, since its spin reorientation should take place above 380 K.¹⁹ The schematic diagram of the spin configuration for $Tb_xDy_{1-x}(Fe_{0.8}Co_{0.2})_2$ ($0.20 \leq x \leq 0.40$) Laves phase is shown in Fig. 6, which is obtained from the collection of the spin-reorientation temperature T_{SR} (anomaly temperature in Fig. 5), the Curie temperature T_C , and the easy magnetization direction EMD. The Curie temperature T_C increases with increasing Tb content, because the Curie temperature of $TbFe_2$ is larger than that of $DyFe_2$. Compared with Terfero-D ($T_C = 653$ K), the Co substitution for Fe increases the Curie temperature T_C and extends their operating temperature scope with about 40 K. It can be seen from Fig. 6 that the spin-reorientation temperature T_{SR} decreases from 365 K for the $Tb_{0.25}Dy_{0.75}(Fe_{0.8}Co_{0.2})_2$ compound to 150 K for the $Tb_{0.4}Dy_{0.6}(Fe_{0.8}Co_{0.2})_2$ compound, when Tb content is increased. The spin-reorientation temperature T_{SR} depends upon the different ratio of Tb/Dy. This is because the Tb^{3+} ion has a negative anisotropy constant K_1 and the EMD of $TbFe_2$ is along $\langle 111 \rangle$, while the Dy^{3+} ion has a positive anisotropy constant K_1 and the EMD of $DyFe_2$ is along $\langle 100 \rangle$ in the entire temperature range.¹⁹ Compared with the $Tb_xDy_{1-x}Fe_2$ system, 20 at. % Co substitution for Fe increases the spin-reorientation temperature T_{SR} and slightly changes the composition for the anisotropy compensation at room temperature to the Tb-rich side. This result is in agreement with the previous reports.^{4,8}

The magnetic field dependence of the magnetization at room temperature for the $Tb_xDy_{1-x}(Fe_{0.8}Co_{0.2})_2$ compounds is shown in Fig. 7. The magnetization for all compounds studied does not vary notably, owing to the fact that the magnetizations at room temperature of $TbFe_2$ and $DyFe_2$ are very close.²⁰ The magnetocrystalline anisotropy constant K_1 of the $Tb_xDy_{1-x}(Fe_{0.8}Co_{0.2})_2$ Laves compounds is determined by simulating the M - H curves using the approximate law of the saturation as follows:²¹

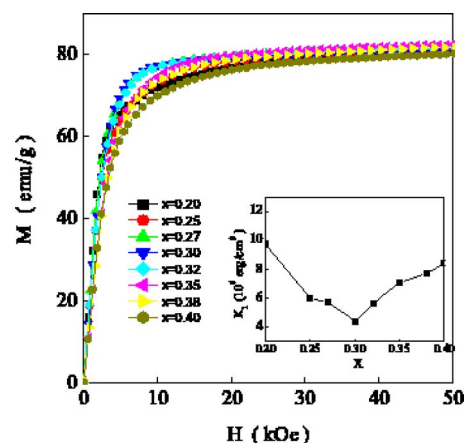


FIG. 7. (Color online) Magnetization curves and the magneto-crystalline anisotropy constant K_1 at room temperature of the $Tb_xDy_{1-x}(Fe_{0.8}Co_{0.2})_2$ compounds.

$$M = M_s \left(1 - \frac{a}{H} - \frac{b}{H^2} \right) + \chi_p H \quad (2)$$

and the relation²¹

$$b = \frac{8}{105} \frac{K_1^2}{\mu_0^2 M_s^2}, \quad (3)$$

where M_s is the saturation magnetization, a and b are constants, and χ_p is the susceptibility of the paramagnetic (parallel) magnetization process. μ_0 is the permeability of free space. The Tb content dependence of the anisotropy constant K_1 is shown in the inset of Fig. 7. The anisotropy constant K_1 decreases with increasing Tb when $0.20 \leq x \leq 0.30$, which can be ascribed to the opposite signs of the anisotropies between Tb^{3+} and Dy^{3+} ions. The anisotropy constant K_1 reaches its minimum at $x=0.30$, which is consistent with the analysis of the XRD and the spin reorientation. The $Tb_{0.30}Dy_{0.70}(Fe_{0.8}Co_{0.2})_2$ compound has a T_{SR} of 285 K, a small magnetocrystalline anisotropy, and a large magneto-

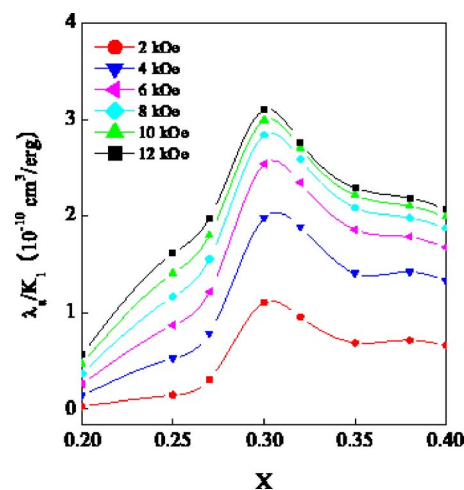


FIG. 8. (Color online) Composition dependence of the ratio λ_a/K_1 for the $Tb_xDy_{1-x}(Fe_{0.8}Co_{0.2})_2$ compounds.

striction λ_s , making it suitable for using a magnetostrictive application at room temperature.

The composition dependence of the ratio λ_a/K_1 for the $\text{Tb}_x\text{Dy}_{1-x}(\text{Fe}_{0.8}\text{Co}_{0.2})_2$ alloys is represented in Fig. 8. It can be seen that every curve presents a peak at $x=0.30$ when the magnetic field varies from 2 kOe to 12 kOe. This result further confirms that the $\text{Tb}_{0.30}\text{Dy}_{0.70}(\text{Fe}_{0.8}\text{Co}_{0.2})_2$ compound has a good property for magnetostriction applications at room temperature.

IV. CONCLUSION

In conclusion, 20 at. % Co substitution for Fe has a strong effect on the magnetic and magnetoelastic properties of the $\text{Tb}_x\text{Dy}_{1-x}\text{Fe}_2$ compounds. Both the Curie temperature and the spin-reorientation temperature are increased by the Co substitution. The EMD at room temperature of $\text{Tb}_x\text{Dy}_{1-x}(\text{Fe}_{0.8}\text{Co}_{0.2})_2$ is in the $\langle 100 \rangle$ direction for $x \leq 0.27$ and changes to the $\langle 111 \rangle$ direction for $x \geq 0.30$. The spin configuration diagram of $\text{Tb}_x\text{Dy}_{1-x}(\text{Fe}_{0.8}\text{Co}_{0.2})_2$

($0.20 \leq x \leq 0.40$) Laves phase has been constructed using the data for T_C , T_{SR} , and EMD. The Co substitution for Fe changes the composition for the anisotropy compensation to the Tb-rich side at room temperature. The large polycrystalline saturation magnetostriction is $\lambda_s \approx 980$ ppm for the $\text{Tb}_{0.30}\text{Dy}_{0.70}(\text{Fe}_{0.8}\text{Co}_{0.2})_2$ compound, which can be ascribed to the large magnetostriction coefficients λ_{111} and λ_{100} . The tetragonal distortion λ_{100} has a positive value larger than 600 ppm for $0.30 \leq x \leq 0.35$, which is ascribed to the filling of the $3d$ band due to the Co substitution for Fe. The polycrystalline compound $\text{Tb}_{0.30}\text{Dy}_{0.70}(\text{Fe}_{0.8}\text{Co}_{0.2})_2$ possesses a high Curie temperature, low anisotropy, and good magnetostrictive properties, which could make it good candidate material for magnetostriction applications.

ACKNOWLEDGMENTS

This work has been supported by the National Natural Science Foundation of China under Grants Nos. 50501021, 50332020, and 59871054.

*Electronic address: wjren@imr.ac.cn

¹A. E. Clark, in *Ferromagnetic Materials*, edited by E. P. Wohlfarth (North-Holland, Amsterdam, 1980), Vol. 1, p. 531.

²A. E. Clark, J. P. Teter, and O. D. McMasters, *IEEE Trans. Magn.* **23**, 3526 (1987).

³K. R. Dhilsha and K. V. Rama Rao, *J. Appl. Phys.* **73**, 1380 (1993).

⁴A. E. Clark, J. P. Teter, and M. Wun-Fogle, *J. Appl. Phys.* **69**, 5771 (1991).

⁵Y. J. Tang, H. L. Luo, N. F. Cao, Y. Y. Liu, and S. M. Pan, *Appl. Phys. Lett.* **66**, 388 (1995).

⁶T. Funayama, T. Kobayashi, I. Sakai, and M. Sahashi, *Appl. Phys. Lett.* **61**, 114 (1992).

⁷T. Y. Ma, C. B. Jiang, X. Xu, H. Zhang, and H. B. Xu, *J. Magn. Mater.* **292**, 317 (2005).

⁸Z. J. Guo, Z. D. Zhang, B. W. Wang, X. G. Zhao, D. Y. Geng, and W. Liu, *J. Phys. D* **34**, 884 (2001).

⁹D. Kendall and A. R. Piercy, *J. Appl. Phys.* **76**, 7148 (1994).

¹⁰M. S. Kumar, K. V. Reddy, and K. V. S. R. Rao, *J. Alloys Compd.* **242**, 70 (1996).

¹¹J. R. Cullen and A. E. Clark, *Phys. Rev. B* **15**, 4510 (1977).

¹²W. J. Ren, Z. D. Zhang, X. P. Song, X. G. Zhao, and X. M. Jin, *Appl. Phys. Lett.* **82**, 2664 (2003).

¹³A. E. Dwight and C. W. Kimball, *Acta Crystallogr., Sect. B: Struct. Crystallogr. Cryst. Chem.* **30**, 2791 (1974).

¹⁴H. Q. Guo, H. Y. Gong, H. Y. Yang, Y. F. Li, L. Y. Yang, B. G. Shen, and R. Q. Li, *Phys. Rev. B* **54**, 4107 (1996).

¹⁵W. J. Ren, Z. D. Zhang, A. S. Markosyan, X. G. Zhao, X. M. Jin and X. P. Song, *J. Phys. D* **34**, 3024 (2001).

¹⁶E. Gratz, A. Lindbaum, A. S. Markosyan, H. Mueller, and A. Y. Sokolov, *J. Phys.: Condens. Matter* **4**, 6699 (1994).

¹⁷N. C. Koon, C. M. Williams, and B. N. Das, *J. Magn. Mater.* **100**, 173 (1991).

¹⁸R. Z. Levitin and A. S. Markosyan, *J. Magn. Mater.* **84**, 247 (1990).

¹⁹U. Atzmony, M. P. Dariel, E. R. Bauminger, D. Lebenbaum, I. Nowik, and S. Ofer, *Phys. Rev. B* **7**, 4220 (1973).

²⁰A. E. Clark, R. Abbundi, and W. R. Gillmor, *IEEE Trans. Magn.* **14**, 542 (1978).

²¹S. Chikazumi, *Physics of Ferromagnetism*, 2nd ed. (Oxford University Press, New York, 1997), p. 503.